Spatial Resolution of the Belle II Silicon Vertex Detector

Soumen Halder[j]*, **H. Aihara**[t], **T. Aziz**[j], **S. Bacher**[x], **S. Bahinipati**[e], **E. Barberio**[a], **Ti. Baroncelli**[a], **To. Baroncelli**[a], **A. K. Basith**[f], **G. Batignani**[k,l], **A. Bauer**[b], **P. K. Behera**[f], **V. Bertacchi**[k,l], **S. Bettarini**[k,l], **B. Bhuyan**[g], **T. Bilka**[d], **F. Bosi**[l], **L. Bosisio**[m,n], **A. Bozek**[x], **F. Buchsteiner**[b], **G. Caria**[a], **G. Casarosa**[k,l], **M. Ceccanti**[l], **D. Červenkov**[d], **T. Czank**[s], **N. Dash**[e], **M. De Nuccio**[k,l], **Z. Doležal**[d], **F. Forti**[k,l], **M. Friedl**[b], **R. Frühwirth**[b], **B. Gobbo**[n], **K. Hara**[u], **T. Higuchi**[p], **C. Irmler**[b], **A. Ishikawa**[s], **C. Joo**[p], **M. Kaleta**[x], **J. Kandra**[d], **K. H. Kang**[v], **P. Kodyš**[d], **T. Kohriki**[u], **I. Komarov**[n], **M. Kumar**[h], **R. Kumar**[i], **P. Kvasnička**[d], **C. La Licata**[m,n], **K. Lalwani**[h], **L. Lanceri**[m,n], **J. Y. Lee**[w], **S. C. Lee**[v], **Y. Li**[c], **J. Libby**[f], **T. Lueck**[k,l], **P. Mammini**[l], **S. N. Mayekar**[j], **G. B. Mohanty**[j], **T. Morii**[p], **K. R. Nakamura**[u], **Z. Natkaniec**[x], **Y. Onuki**[t], **W. Ostrowicz**[x], **A. Paladino**[p], **E. Paoloni**[k,l], **H. Park**[v], **K. Prasanth**[j], **A. Profeti**[l], **K. K. Rao**[j], **I. Rashevskaya**[A, n], **P. K. Resmi**[f], **G. Rizzo**[k,l], **M. Rozanska**[x], **D. Sahoo**[j], **N. Sato**[u], **S. Schultschik**[b], **C. Schwanda**[b], **J. Stypula**[x], **J. Suzuki**[u], **S. Tanaka**[u], **H. Tanigawa**[t], **G. N. Taylor**[a], **R. Thalmeier**[b], **T. Tsuboyama**[u], **P. Urquijo**[a], **M. Watanabe**[q], **S. Watanuki**[s], **I. J. Watson**[t], **J. Webb**[a], **J. Wiechczynski**[x], **S. Williams**[a], **H. Yin**[b] and **L. Zani**[k,l]

(Belle II SVD Group)
[a]School of Physics, University of Melbourne, Melbourne, Victoria 3010, Australia
[b]Institute of High Energy Physics, Austrian Academy of Sciences, 1050 Vienna, Austria
[c]Peking University, Department of Technical Physics, Beijing 100871, China
[d]Faculty of Mathematics and Physics, Charles University, 121 16 Prague, Czech Republic
[e]Indian Institute of Technology Bhubaneswar, Satya Nagar, India
[f]Indian Institute of Technology Madras, Chennai 600036, India
[g]Indian Institute of Technology Guwahati, Assam 781039, India
[h]Malviya National Institute of Technology, Jaipur 302017, India
[i]Punjab Agricultural University, Ludhiana 141004, India
[j]Tata Institute of Fundamental Research, Mumbai 400005, India
[k]Dipartimento di Fisica, Università di Pisa, I-56127 Pisa, Italy
[l]INFN Sezione di Pisa, I-56127 Pisa, Italy
[m]Dipartimento di Fisica, Università di Trieste, I-34127 Trieste, Italy
[n]INFN Sezione di Trieste, I-34127 Trieste, Italy
[o]Presently at TIFPA-INFN, Dipartimento di Fisica, Universit di Trento, I-38123 Trento, Italy
[p]Kavli Institute for the Physics and Mathematics of the Universe (WPI), University of Tokyo, Kashiwa 277-8583, Japan
[q]Department of Physics, Niigata University, Niigata 950-2181, Japan
[r]Presently at Nippon Dental University, Niigata 951-8580, Japan
[s]Department of Physics, Tohoku University, Sendai 980-8578, Japan
[t]Department of Physics, University of Tokyo, Tokyo 113-0033, Japan
[u]High Energy Accelerator Research Organization (KEK), Tsukuba 305-0801, Japan
[v]Department of Physics, Kyungpook National University, Daegu 702-701, Korea
[w]Department of Physics and Astronomy, Seoul National University, Seoul 151-742, Korea
[x]H. Niewodniczanski Institute of Nuclear Physics, Krakow 31-342, Poland
E-mail: soumen.halder@tifr.res.in

The Belle II experiment at the SuperKEKB collider in Japan will search for new sources of CP violation as well as probe new physics by studying the suppressed decays of beauty and charm mesons. In these pursuits, the spatial resolution of the silicon vertex detector (SVD) of the experiment will play a key role. We report here the spatial resoution of SVD sensors using data simulated with the Phase-2 geometry.

---

*Speaker.

1. Introduction

Belle II at SuperKEKB will search for new sources of CP violation and probe new physics by studying the suppressed decays of beauty and charm mesons. The experiment is located at an interaction point of the SuperKEKB e^+e^- collider, which is operating at a center-of-mass energy near the $\Upsilon(4S)$ resonance, in Tsukuba, Japan. The positron and electron beam have unequal energies of 4 and 7 GeV, respectively, which make the $\Upsilon(4S)$ boosted with a Lorentz factor $\beta\gamma = 0.28$ in the laboratory frame. The SuperKEKB, an upgraded version of KEKB, aims to deliver collision data at an unprecedented luminosity of 8×10^{35} cm^{-2}s^{-1}, 40 times higher than its predecessor, by a sizable decrease in the beam cross section and a moderate increase in the beam current.

The reconstruction of charged particles near the interaction point is provided by a six-layer VerteX Detector (VXD), which consists of two layers of PiXel Detector (PXD) at radii 1.4 and 2.2 cm, surrounded by four layers of Silicon Vertex Detector (SVD) at radii 3.8, 8.0, 11.5 and 14.0 cm. The PXD and SVD comprised of DEpleted P-channel Field Effect Transistor (DEPFET) pixel sensors and Double-sided Silicon Strip Detectors (DSSDs), respectively. At Belle II, the precise determination of decay vertex and low-momentum tracking are crucial to indirectly probe new physics. The VXD is designed to have an excellent spatial resolution ($\sim$20 μm) to efficiently perform this job.

2. The Silicon Vertex Detector

The Belle II SVD consists of ladders that are basically an array of DSSD sensors. Layer-3, 4, 5 and 6 having 7, 10, 12 and 16 ladders, respectively, are cylindrically arranged around the interaction point. Layer 1 and 2 are the two PXD layers. To minimize material budget while at the same time to cover a polar angle range $17° < \theta < 150°$, where θ is the angle measured from the interaction point with respect to the beam (or z) axis, the last DSSDs of all ladders of Layer-4, 5 and 6 are slanted with an angle of 11.9°, 16.0° and 21.1°, respectively. Each DSSD is either rectangular or trapezoidal having $300 - 320$ μm thickness with n-type bulk whose one side is doped by acceptor (called strips) and the other side is doped by donor, with strips being perpendicular to the former. The acceptor implanted side, called p or U side, having longer strips parallel to the length of the sensor, measure the $r - \phi$ coordinate. The donor implanted (n or V side) shorter strips measure the z coordinate. The sensors have readout pitch varying between 50–75 μm in the $r - \phi$ plane and 160–240 μm along the z axis. To improve the spatial resolution, one floating strip is implemented between two readout strips. A detailed description of the SVD can be found in Ref. [1].

3. Phase-2 Monte Carlo Samples

A partial VXD, with one ladder per layer for all six layers, installed along with all other sub-detectors has recorded about 500 pb^{-1} of e^+e^- collision data during February–June 2018. This running cycle is called Phase-2 run. Figure 1 shows the layout of Phase-2 SVD. Approximately 5 million $e^+e^- \to \mu^+\mu^-$ Monte Carlo (MC) events generated and simulated with the beam background environment appropriate for Phase-2 are used in the analysis.
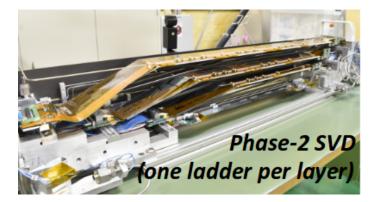
Figure 1: Layout of the Phase-2 SVD with one ladder per layer. Going from outward to inward, one can see layer-6, 5 and 4 (layer-3 and PXD layers are barely visible).

4. Measurement of Spatial Resolution

The spatial resolution of the SVD is nothing but the uncertainty associated to hit position (σ_{hit}). It can be extracted from the overall residual distribution where residual is the difference between the measured hit position and the position of track extrapolated to the sensor plane. Since the latter has an overall uncertainty (σ_{track}) associated with it, σ_{hit} is calculated as the square root of the quadrature difference between σ_{total} and σ_{track} i.e., $\sigma_{\text{hit}} = \sqrt{(\sigma_{\text{total}})^2 - (\sigma_{\text{track}})^2}$, where σ_{total} is the width of a sum of two Gaussian functions fitted to the residual distribution. The statistical uncertainty associated to σ_{hit} is $\sqrt{\left[\frac{\sigma_{\text{total}}}{\sigma_{\text{hit}}}\delta(\sigma_{\text{total}})\right]^2 + \left[\frac{\sigma_{\text{track}}}{\sigma_{\text{hit}}}\delta(\sigma_{\text{track}})\right]^2}$ with $\delta(\sigma_{\text{total}})$ and $\delta(\sigma_{\text{track}})$ being obtained from the fitting.

For the above dimuon MC sample we extract σ_{track} using MC information. Basically we fit the true residual distribution to the sum of two Gaussian functions and take its effective width as σ_{track}.

To remove potential bias, the track is fitted without using hits of the SVD layer under study. Two additional requirements are imposed for selecting the track: the hits associated with the track must contain at least one layer PXD hit and at least one layer SVD hit. Similar discussion can be found in Ref. [2].

Some examples of residual and true-residual plots are given below. Figures 2 and 4 correspond to the true-residual plots while Figures 3 and 5 denote the residual plots.

Layer	Sensor	Side	Readout pitch (p) in μm	Digital resolution $= \frac{p}{2\sqrt{12}}$ in μm	σ_{hit} in μm for cluster size	
					one	two
3	2	U	50	7.21	5.78±0.09	5.02±0.09
3	2	V	160	23.09	17.86±0.08	14.66±0.15
4	2	U	75	10.82	10.01 ±0.09	6.58±0.08
4	2	V	240	34.64	26.83±0.17	19.07±0.24
5	3	U	75	10.82	10.29±0.14	7.01±0.15
5	3	V	240	34.64	27.06±0.23	19.22±0.36
6	3	U	75	10.82	11.56±0.37	8.52±0.34
6	3	V	240	34.64	27.16±1.38	20.86±0.67

Table 1: Spatial resolutions for different sensors of layer 3–6 for both U and V sides. Cluster size one means the hit position is reconstructed from one flagged strip and the corresponding hit resolution should match with the digital resolution as no charge sharing has taken place. Due to charge sharing the hit resolution for cluster size two should be better than that of cluster size one. The factor of 2 in the digital resolution expression takes into account that there is one floating strip between two readout strips.
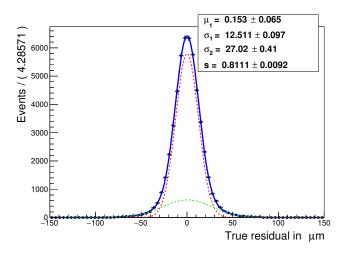

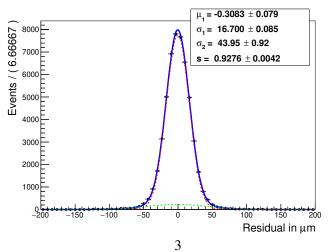**Figure 2:** True residual distribution for the 6th layer 3rd sensor U-side with cluster size one.

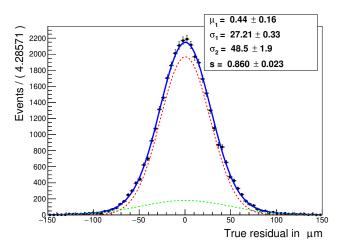**Figure 3:** Residual distribution for the 6th layer 3rd sensor U-side with cluster size one.

Figure 4: True Residual distribution for the 6rd layer 3rd sensor V-side with cluster size one.
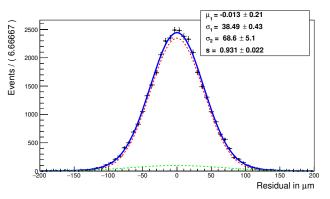

Figure 5: Residual distribution for the 6rd layer 3rd sensor V-side with cluster size one.

Smaller cluster position residuals on the U side reflect the smaller strip pitch as well as a better estimation of track parameters along the U side compared to the V side due to the drift chamber geometry.

5. Summary

We have found that the spatial resolution for single strip cluster is better than the digital resolution. Due to charge sharing the spatial resolution for multi-strip cluster is better than single strip cluster.

References

[1] T. Abe et al., *Belle II Technical Design Report*, `arXiv:1011.0352`.

[2] T. Lueck et al., `PoS VERTEX 2016 (2016) 056`.